Electron-phonon coupling and phonon self-energy in MgB_2: Interpretation of MgB_2 Raman spectra

Matteo Calandra and Francesco Mauri
Laboratoire de Minéralogie-Cristallographie, case 115, 4 Place Jussieu, 75252 Paris cedex 05, France
(Received 3 June 2004; revised manuscript received 9 November 2004; published 1 February 2005)

We consider a model Hamiltonian fitted on the *ab initio* band structure to describe the electron-phonon coupling between the electronic σ bands and the phonon E_{2g} mode in MgB_2. The model allows for analytical calculations and numerical treatments using very large k-point grids. We calculate the phonon self-energy of the E_{2g} mode along two high symmetry directions in the Brillouin zone. We demonstrate that the contribution of the σ bands to the Raman linewidth (Landau damping) of the E_{2g} mode via the electron-phonon coupling is zero. As a consequence the large resonance seen in Raman experiments cannot be interpreted as originated from the E_{2g} mode at Γ. We examine in details the effects of Fermi surface singularities in the phonon spectrum and linewidth and we determine the magnitude of finite temperature effects in the phonon self-energy. From our findings we suggest several possible effects which might be responsible for the MgB_2 Raman spectra.

DOI: 10.1103/PhysRevB.71.064501 PACS number(s): 74.70.Ad, 63.20.Kr, 63.20.Dj, 78.30.Er

I. INTRODUCTION

The knowledge of the MgB_2 (Ref. 1) electronic structure allows us to obtain a qualitative understanding of several peculiar features of this material. A crucial role is played by the σ bands,[2–4] formed by the in-plane boron-boron *sp* bonding. Due to the small interlayer coupling between the boron layers, these bands have a two dimensional character and are weakly dispersing along the ΓA direction. Their corresponding Fermi surface sheets[4] are two slightly warped cylinders, with axis perpendicular to the Boron layers. This peculiar topology results in a large contribution to the real and imaginary parts of the phonon self-energy of the E_{2g} phonon mode, an in plane displacement of the boron atoms.

The large contribution to the real part of the phonon self-energy has spectacular consequences on the phonon spectrum: the phonon frequencies of the E_{2g} modes undergo a reduction of roughly 20 meV along the ΓA directions as predicted by *ab initio* calculations[5–7] and measured by high-energy inelastic x-ray scattering.[7,8] Density functional theory calculations of phonon[5–7] spectra indicate that the softening of the E_{2g} phonon frequencies when approaching the ΓA direction, even if strong in magnitude, is not as abrupt as would be expected[9] for a pure two-dimensional system having a Kohn anomaly. The experimental phonon dispersion[7] along AL and ΓM (Refs. 7 and 8) confirms that the E_{2g} phonon frequencies decrease gradually as the ΓA direction is approached and the softening at momenta corresponding to the cylinders $2k_F$ is very small. The Kohn anomaly might indeed be mitigated by the presence of a k_z band dispersion and a finite temperature. In this paper we investigate the magnitude of these two effects and discuss their relevance in the interpretation of experimental data.

A large contribution due to the electron-phonon coupling is also associated with the imaginary part of the E_{2g} phonon self-energy, the phonon linewidth. Inelastic x-ray scattering experiments and theoretical calculations[7,8] show an anomalously large broadening [$\sim$20–30 meV full width at half maximum (FWHM)] of the E_{2g} mode along the ΓA direction only. According to Ref. 8 the broadening of this mode is almost temperature independent, but the spectra displayed in Fig. 4 of Ref. 8 do not allow for a definitive conclusion since the E_{2g} mode has a very small structure factor and it is seen only as a shoulder of the close E_{1u} mode.

Raman data show a completely different behavior. Raman experiments probe excitations at small momentum transfer, close to the Γ point of the material. The maximum momentum transfer is $q_{\rm exp}=2q_{\rm light}$ where $q_{\rm light}=2\pi/\lambda$ and λ is the wavelength of the incident light. Most of the experiments are performed with a 514.5 nm (2.41 eV) argon laser[10] which corresponds to $q_{\rm exp}=1.3\times10^{-3}a_0^{-1}$ ($a_0=0.5292$ Å is the Bohr radius). This estimate is further reduced due to the presence of a finite skin depth in the material.[11] The skin depth is about $944.8a_0$,[12] leading to $q_{\rm exp}^{sd}=1.3\times10^{-2}$. This region is inaccessible to x-ray measurement and as a consequence a direct experimental comparison between the two techniques cannot be performed. Nevertheless it is instructive to compare Raman spectra with the x-ray data as close as possible to the Γ point.

Below T_c, the MgB_2 Raman spectra show two prominent features. A low-energy one at $\approx$12.5 meV (Ref. 10) related to the breaking of Cooper pairs in the superconducting state[13] and a second one at $\approx$77 meV which is commonly attributed to the E_{2g} phonon mode at the Γ point[10,14–19] (the E_{2g} mode is the only Raman active mode in MgB_2). For temperatures higher than T_c, only the 77 meV feature is left. In this work we focus on the normal state Raman spectra and consequently we only consider the 77 meV feature at $T>T_c$. The linewidth of the 77 meV feature[10,14–19] shows a very strong temperature dependence since it is $\sim$20 meV (FWHM) at 40 K and reaches almost 40 meV at room temperature, a factor of 2 larger than the one detected in inelastic x-ray data along the ΓA direction. Since, according to the calculation performed in Ref. 7, the anharmonic broadening at room temperature is 1.2 meV, it cannot be responsible of neither the large linewidth nor of its strong temperature dependence.

An unexplored cause of such a large temperature dependence of the linewidth might be the electron-phonon cou-

pling. The electron-phonon coupling contribution to the phonon linewidth is indeed temperature dependent [see Eq. (4), this work]. Nevertheless the dependence on temperature is usually assumed to be negligible, but no detailed studies have been performed on the subject.

In this work we carefully analyze all the approximations involved in the calculation of the phonon linewidth due to the electron-phonon coupling. We analyze the temperature dependence of the phonon linewidth and the effects of neglecting the phonon frequency in the Allen formula. It would be highly desirable to estimate the magnitude of these approximations using *ab initio* calculation, but the task is almost prohibitive. In actual *ab initio* calculations[5,7] a finite number of k points is used together with a ~ 0.025 Ry (~ 3000 K) smearing of the Fermi surface.[20] Physical effects involving temperature difference between 40 and 300 K are basically invisible to the calculation, since grids having at least 1000 times larger number of k points would be needed.[21] In this case, the calculated electron-phonon coupling contributions and its temperature dependence in the indicated region would be masked by computational details. The convergence of *ab initio* calculations with the number of symmetry-irreducible k points is particularly relevant for MgB_2,[22] since only the weak warping of the two cylindrical σ bands Fermi surface sheets prevents the linewidth from diverging. Moreover, if there were effects such as anomalies in phonon spectra generated by the $2k_F$ singularities,[8] they could be detected only using a very large number of k points in the phonon frequencies calculations. As a consequence the use of a too small k points mesh might affect the calculation of both the real and imaginary part of the phonon self-energy.

For these reasons, in this work we study the behavior of the phonon self-energy of the E_{2g} mode due to the electron-phonon interaction between this mode and the σ bands using a model Hamiltonian. The Hamiltonian is composed by the two σ bands coupled to an harmonic dispersionless E_{2g} phonon mode. The form considered for the σ bands is fitted from *ab initio* calculations[5] in the region close to the Γ point. The phonon frequency is that of the E_{2g} at Γ. The model is illustrated in detail in Sec. II, together with the form of the phonon self-energy in its real (phonon shift) and imaginary (phonon linewidth) parts. The simplified form of the model allows to calculate analytically the linewidth as $\mathbf{q}\rightarrow\Gamma$ along any high symmetry direction. Moreover it allows numerical calculations using grids of $N_k = 300\times 300\times 300$, symmetry-irreducible k points in any point of the Brillouin zone, which are enough to see temperature effects in the phonon linewidth due to the electron-phonon coupling.

In Sec. III we calculate the phonon linewidth *exactly* in the limit $\mathbf{q}\rightarrow\Gamma$ both in its intraband and in its σ-σ interband contributions. We consider two cases, (i) $\mathbf{q}$ along the ΓA direction (Sec. III A) and (ii) $\mathbf{q}$ along ΓM, or generally along any direction in the (k_x, k_y) plane (Sec. III B), since the bands and the considered coupling are isotropic in the (k_x, k_y) plane. We discuss the relevance of the results for the interpretation of Raman spectra.

In Sec. IV we follow Ref. 23 and derive the Allen formula starting from the phonon self-energy, paying particular attention at the approximations involved. Subsequently in Sec. V we numerically evaluate the phonon self-energy along the ΓA and ΓM directions for the case of a k-independent electron-phonon coupling. We estimate the effects of temperature and of σ-σ interband transitions. We evaluate the magnitude of the different approximations involved in the derivation of the Allen formula. The numerical results are also used as benchmarks to judge the reliability of the preceding *ab initio* calculations[7] performed with a smaller number of k points and a larger smearing parameter. Finally we question the attribution of the 77 meV peak to the E_{2g} mode and we suggest other interpretation of the Raman experiments.

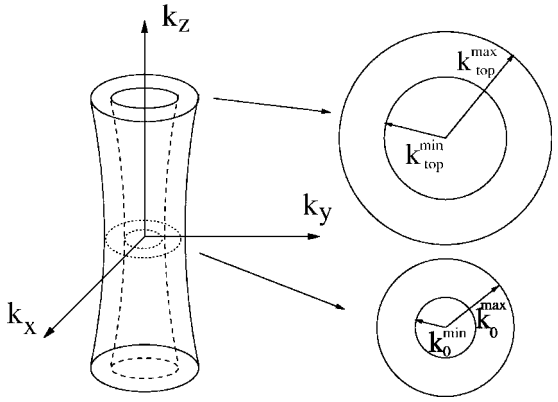

FIG. 1. σ-band Fermi surface cylinders with projection over the $k_z=\pi/c$ and $k_z=0$ planes.

II. MODEL

Following Ref. 5, the structure of the σ bands close to the Fermi energy can be expressed as

$$\epsilon_{\mathbf{k}n} = \epsilon_0 - 2t_\perp \cos(k_z c) - \frac{k_x^2 + k_y^2}{M_n}\mathcal{R}y, \tag{1}$$

where the index n label the heavy/light hole bands. The holes masses are $M_1=0.59$ (heavy holes), $M_2=0.28$ (light holes). The average energy along ΓA, $t_\perp=0.094$ eV, gives the dispersion of the bands. The top of the σ bands is $\epsilon_0=0.58$ eV. Note that k are expressed in atomic units and $(k^2/M)\mathcal{R}y$ in eV with $\mathcal{R}y=13.605$. The bands are measured with respect to the Fermi energy. The Fermi surface sheets identified by the bands in Eq. (1) are two warped cylinders (see Fig. 1). The radii in the $k_z=0$ plane are $k_0^{\max}=0.13\ a_0^{-1}$ and $k_0^{\min}=0.09\ a_0^{-1}$. The radii in the $k_z=\pm\pi/c$ planes are $k_{\text{top}}^{\max}=0.18\ a_0^{-1}$ and $k_{\text{top}}^{\min}=0.126\ a_0^{-1}$.

Neglecting vertex corrections,[24] the contribution to the ν phonon mode phonon self-energy due to the electron phonon coupling can be written as

$$\Pi_\nu(\mathbf{q},\omega_{\mathbf{q}\nu}) = \frac{2}{N_k}\sum_{\mathbf{k},m,n} |g^\nu_{\mathbf{k}n,\mathbf{k}+\mathbf{q}m}|^2 \frac{f_{\mathbf{k}+\mathbf{q}m} - f_{\mathbf{k}n}}{\epsilon_{\mathbf{k}+\mathbf{q}m} - \epsilon_{\mathbf{k}n} - \omega_{\mathbf{q}\nu} - i\eta}, \tag{2}$$

where N_k is the number of k points, the sum is over the Brillouin zone and $f_{\mathbf{k}n}$ are the Fermi distribution functions.

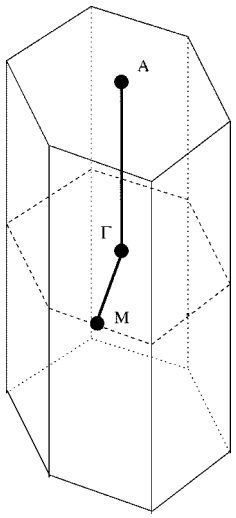

FIG. 2. MgB_2 Brillouin zone with high symmetry points and directions considered in the paper.

The matrix element is $g^{\nu}_{\mathbf{k}n,\mathbf{k}+\mathbf{q}m}=\langle \mathbf{k}n|\delta V/\delta u_{\mathbf{q}\nu}|\mathbf{k}+\mathbf{q}m\rangle/\sqrt{2\omega_{\mathbf{q}\nu}}$, where $u_{\mathbf{q}\nu}$ is the amplitude of the displacement of the phonon ν of wave vector $\mathbf{q}$, $\omega_{\mathbf{q}\nu}$ its phonon frequency and V the electron-ion interacting potential.[25]

The real part of the phonon self-energy is

$$\frac{\Delta_q}{2}=\frac{2}{N_k}\sum_{\mathbf{k},m,n}|g^{\nu}_{\mathbf{k}n,\mathbf{k}+\mathbf{q}m}|^2\mathcal{P}\left[\frac{f_{\mathbf{k}+\mathbf{q}m}-f_{\mathbf{k}n}}{\epsilon_{\mathbf{k}+\mathbf{q}m}-\epsilon_{\mathbf{k}n}-\omega_{\mathbf{q}\nu}}\right], \tag{3}$$

where $\mathcal{P}$ stands for the principal value. With this definition, Δ_q express the renormalization of the harmonic phonon frequencies due to electron-phonon coupling effects.

The phonon linewidth (FWHM) is twice the imaginary part of $\Pi_{\nu}(\mathbf{q},\omega_{\mathbf{q}\nu})$ divided by N_k, as it can also be inferred from Fermi golden rule:

$$\gamma_{\mathbf{q}\nu}=\frac{4\pi}{N_k}\sum_{\mathbf{k},m,n}|g^{\nu}_{\mathbf{k}n,\mathbf{k}+\mathbf{q}m}|^2(f_{\mathbf{k}n}-f_{\mathbf{k}+\mathbf{q}m})\delta(\epsilon_{\mathbf{k}+\mathbf{q}m}-\epsilon_{\mathbf{k}n}-\omega_{\mathbf{q}\nu}). \tag{4}$$

In the following two subsections we calculate the phonon linewidth in the limit $\mathbf{q}\to 0$ analytically. We use formula Eq. (4) choosing $\mathbf{q}$ along two high symmetry directions in the Brillouin zone: (i) the out of plane ΓA directions and (ii) the in-plane ΓM direction (see Fig. 2). We show that in both cases the phonon linewidth vanishes in the $\mathbf{q}\to 0$ limit.

III. MgB_2 RAMAN LINEWIDTH

A. Γ*A* direction

We choose $\mathbf{q}$ along the ΓA direction and consider the limit for $\mathbf{q}$ going to zero:

$$\epsilon_{\mathbf{k}+\mathbf{q}m}=\epsilon_{\mathbf{k}n}-\frac{k_{\parallel}^2}{M_n}\left(\frac{M_n}{M_m}-1\right)\mathcal{R}y+2t_{\perp}qc\,\sin(k_zc), \tag{5}$$

where $k_{\parallel}^2=k_x^2+k_y^2$. Equation (5) is correct at order $O(q^2)$. Choosing $\omega_{\mathbf{q}\nu}=65$ meV (i.e., the harmonic E_{2g} phonon frequency at Γ) and substituting in Eq. (2) we get

$$\gamma_{\mathbf{q}\nu}=\frac{4\pi}{N_k}\sum_{\mathbf{k}m,n}|g^{\nu}_{\mathbf{k}n,\mathbf{k}+\mathbf{q}m}|^2(f_{\mathbf{k}+\mathbf{q}m}-f_{\mathbf{k}n}) \times\delta\left[\frac{k_{\parallel}^2}{M_n}\left(\frac{M_n}{M_m}-1\right)\mathcal{R}y-2t_{\perp}qc\,\sin(k_zc)+\omega_{\mathbf{q}\nu}\right]. \tag{6}$$

This sum can be divided in two different contributions, one coming from intraband transitions ($m=n$) and the other from interband transitions ($m\neq n$).

If $n=m$ and in the limit of $\mathbf{q}\to 0$, in Eq. (6) in order for the δ function to be satisfied we must have that $\omega_{\mathbf{q}\nu}=2t_{\perp}qc\,\sin(k_zc)$. The momentum used in Raman experiment[10] $q_{\mathrm{exp}}=1.3\times10^{-3}a_0^{-1}$. Raman scattering then samples a sphere in momentum space centered at Γ and of radius q_{exp}. It follows then that

$$|2t_{\perp}q_{\mathrm{exp}}c|=1.6\ \mathrm{meV}\ll\omega_{\mathbf{q}\nu}=65\ \mathrm{meV} \tag{7}$$

using $c=6.653a_0$. Thus the δ-function condition in Eq. (6) is never fulfilled in Raman experiments. The contribution to the linewidth due to intraband transition is then exactly zero. The general fact that an optical phonon mode cannot couple with electrons at Γ as long as only intraband transitions are allowed has already been noted in Refs. 26–29.

Choosing a finite q along ΓA and using Eq. (7) we can determine the values of q in the Brillouin zone for which the intraband contribution is nonzero, namely,

$$q\geqslant q^{\mathrm{intra}}=\frac{\omega_{\mathbf{q}\nu}}{2t_{\mathrm{perp}}c}\approx 0.052\ a_0^{-1}\approx 0.1\Gamma A. \tag{8}$$

In this estimate we have used the phonon frequency of the E_{2g} at Γ, as the phonon branches are fairly flat along ΓA and $\mathbf{q}\to 0$. We have also assumed the expansion (5) at order $O(q^2)$ to be correct. We will show in Sec. V B that this limit is indeed correct using numerical calculation.

We then consider the interband contributions ($m\neq n$) and $\mathbf{q}\to\Gamma$. In order for the argument of the delta function in Eq. (6) to be satisfied we must have that

$$2t_{\perp}qc\,\sin(k_zc)-\frac{k_{\parallel}^2}{M_n}\left(\frac{M_n}{M_m}-1\right)\mathcal{R}y=\omega_{\mathbf{q}\nu}. \tag{9}$$

In the case $n=1$ and $m=2$, we have $(M_1/M_2-1)>0$ since $M_1>M_2$. As a consequence the largest value of $\mathbf{q}$ for which the delta function is nonzero is determined by the condition

$$|2t_{\perp}qc|<\omega_{\mathbf{q}\nu} \tag{10}$$

which leads to the same condition as in the intraband transitions case, namely,

$$q\geqslant 0.1\Gamma A. \tag{11}$$

Then we consider the term with $n=2$ and $m=1$. In order for Eq. (6) to give a finite linewidth at $T=0$ K, the following two conditions must be simultaneously satisfied: (i) the states ϵ_{k1} are occupied and the states ϵ_{k2} empty (and vice versa) and (ii) the delta function in Eq. (6) must be satisfied. Recalling the Fermi surface topology of the two σ bands, the first condition means that the sum is limited to the region of space

included between the two warped cylinders. This region is included between the two cylinders having axes along ΓA and radii $k_0^{\min}$ and $k_{\text{top}}^{\max}$, respectively. On the other hand, for the second condition to be fulfilled we must have

$$|q| \geqslant \frac{k_\parallel^2}{M_2}\frac{0.525\mathcal{R}y}{2t_\perp c} + \frac{\omega_{\mathbf{q}\nu}}{2t_\perp c}, \tag{12}$$

where we have substituted $(M_2/M_1-1)=-0.525$. The constraint imposed by the two Fermi functions [condition (i)] allows one to replace $k_\parallel$ with $k_0^{\min}$ in the inequality

$$|q| \geqslant \frac{(k_0^{\min})^2}{M_2}\frac{0.525\mathcal{R}y}{2t_\perp c} + \frac{\omega_{\mathbf{q}\nu}}{2t_\perp c} > \frac{\omega_{\mathbf{q}\nu}}{2t_\perp c} \approx 0.1\Gamma A. \tag{13}$$

From Eq. (13) we conclude that even the term with $n=2$ and $m=1$ in Eq. (6) is zero for $|q|<0.1\Gamma A$ (threshold for Landau damping). A similar equation can be derived for the case $\epsilon_{\mathbf{k}1}>0$ and $\epsilon_{\mathbf{k}+\mathbf{q}2}<0$, so that intraband transitions give no contribution to the Raman linewidth.

We have shown that both the σ bands intraband and interband contributions to the phonon linewidth via the electron-phonon interaction are zero for $\mathbf{q}$ along ΓA and

$$|q| < 0.1\Gamma A \approx 0.052\ a_0^{-1}. \tag{14}$$

B. In-plane momenta

We now choose $\mathbf{q}$ in the k_x,k_y plane and consider the limit for $\mathbf{q}$ going to zero, we have that

$$\epsilon_{\mathbf{k}+\mathbf{q}m} = \epsilon_{\mathbf{k}n} - \frac{|k_\parallel+q|^2}{M_m}\mathcal{R}y + \frac{|k_\parallel|^2}{M_n}\mathcal{R}y, \tag{15}$$

where we have chosen $\mathbf{q}$ along the ΓM direction. The phonon linewidth becomes

$$\gamma_{\mathbf{q}\nu} = \frac{4\pi}{N_k}\sum_{\mathbf{k}m,n}|g^\nu_{\mathbf{k}n,\mathbf{k}+\mathbf{q}m}|^2(f_{\mathbf{k}+\mathbf{q}m}-f_{\mathbf{k}n}) \times\delta\left[-\frac{|\mathbf{k}_\parallel+\mathbf{q}|^2}{M_m}\mathcal{R}y + \frac{|\mathbf{k}_\parallel|^2}{M_n}\mathcal{R}y + \omega_{\mathbf{q}\nu}\right]. \tag{16}$$

We neglect terms of order q^2. We first consider intraband transition only $(m=n)$. In this case, we obtain

$$\gamma^{\text{intra}}_{\mathbf{q}\nu} = \frac{4\pi}{N_k}\sum_{\mathbf{k}m}|g^\nu_{\mathbf{k}m,\mathbf{k}+\mathbf{q}m}|^2(f_{\mathbf{k}+\mathbf{q}m}-f_{\mathbf{k}m})\delta\left(\omega_{\mathbf{q}\nu}-\frac{2qk_x}{M_m}\mathcal{R}y\right), \tag{17}$$

where k_x is along ΓM. In order for Eq. (17) to give a nonzero value for $\gamma_{\mathbf{q}\nu}$ the δ function must be satisfied so that $2qk_x\mathcal{R}y=M_m\omega$. The two Fermi functions limit the sum in the regions of space with (i) $\epsilon_{\mathbf{k}m}<0$ and $\epsilon_{\mathbf{k}+\mathbf{q}m}>0$ and (ii) $\epsilon_{\mathbf{k}m}>0$ and $\epsilon_{\mathbf{k}+\mathbf{q}m}<0$. In case (i) the sum over $\mathbf{k}$ is limited to the region included by one of the two cylinders, depending on the value of the index m. The maximum k possible is $k^{(1)}_{\max}=k^{\max}_{\text{top}}$ for $m=1$ and $k^{(2)}_{\max}=k^{\min}_{\text{top}}$ for $m=2$. We can then substitute $k^{(1)}_{\max}$ and $k^{(2)}_{\max}$ in the δ-function condition in Eq. (17) to obtain $q_1=7.8\times10^{-3}a_0^{-1}\approx0.0125\Gamma M$ for $m=1$ and $q_2=5.3\times10^{-3}a_0^{-1}\approx0.0085\Gamma M$ for $m=2$. In case (ii) the sum is limited to the region of space outside one of the two cylinders and, since $\epsilon_{\mathbf{k}+\mathbf{q}m}<0$ then $q>k_\parallel-k^{\max}_{\text{top}}$ for $m=1$ and $q>k_\parallel-k^{\min}_{\text{top}}$ for $m=2$, with $q>0$ in both cases. Inserting $q=k_\parallel-k^{\max}_{\text{top}}$ or $q=k_\parallel-k^{\min}_{\text{top}}$ in the δ-function condition and solving for k_x one gets $q_1'=7.4\times10^{-3}a_0^{-1}\approx0.012\Gamma M$ for $m=1$ and $q_2'=5.1\times10^{-3}a_0^{-1}\approx0.008\Gamma M$ for $m=2$. Finally the intraband contribution vanishes completely for $|\tilde{q}|<|q|<q_{\text{intra}}=\min\{q_1,q_2,q_1',q_2'\}=5.1\times10^{-3}a_0^{-1}$, which is factor of 4 larger than the exchanged momentum $q_{\text{exp}}=1.3\times10^{-3}a_0^{-1}$ in Raman scattering.

Note that this conservative estimate has been obtained using the E_{2g} phonon frequency at Γ. In the (k_x,k_y) plane the E_{2g} phonon modes are not degenerate and both have phonon frequencies which are larger than the value at Γ.[7] The use of a larger $\omega_{\mathbf{q}\nu}$ would lead to the vanishing of the phonon linewidth at a larger value of $\mathbf{q}$.

Then we consider the interband case $(m\neq n)$. We start considering $n=1$ and $m=2$. In order for the Fermi function difference in Eq. (16) to be nonzero one of the following conditions must be satisfied: (i) $\epsilon_{k1}>0$ and $\epsilon_{k+q2}<0$, (ii) $\epsilon_{k1}<0$ and $\epsilon_{k+q2}>0$. The first condition means that $|q|>k_0^{\max}-k_0^{\min}\approx0.04a_0^{-1}=0.064\Gamma M$ (the $k_z=0$ plane is where the surfaces of the two cylinders are closer), i.e., no contribution to the linewidth for momenta smaller than $0.064\Gamma M$.

The second condition leads to $k_\parallel<k_0^{\max}$ and $|\mathbf{k}_\parallel+\mathbf{q}|>k_0^{\min}$. Thus we have

$$\frac{|k_\parallel+q|^2}{M_2}\mathcal{R}y > \frac{(k_0^{\min})^2}{M_2}\mathcal{R}y > \frac{(k_0^{\max})^2}{M_1}\mathcal{R}y \tag{18}$$

meaning that the δ-function condition

$$\frac{|k_\parallel+q|^2}{M_2}\mathcal{R}y + \omega_{\mathbf{q}} = \frac{|k_\parallel|^2}{M_1}\mathcal{R}y \tag{19}$$

is never satisfied. Then we consider the case $n=2$, $m=1$. The Fermi functions in Eq. (16) give the following two conditions: (i) $\epsilon_{\mathbf{k}2}<0$ and $\epsilon_{\mathbf{k}+\mathbf{q}1}>0$, (ii) $\epsilon_{\mathbf{k}2}>0$ and $\epsilon_{\mathbf{k}+\mathbf{q}1}<0$. In case (i) we have that $k_\parallel<k_0^{\min}$ and $|\mathbf{k}+\mathbf{q}|>k_0^{\max}$ and we get the same result of $n=1$, $m=2$ case (i). In case (ii) we have $k_\parallel>k_0^{\min}$ and $|\mathbf{k}+\mathbf{q}|<k_0^{\max}$. We have

$$\frac{k_\parallel^2}{M_2}\mathcal{R}y > \frac{(k_0^{\min})^2}{M_2}\mathcal{R}y > \frac{(k_0^{\max})^2}{M_1}\mathcal{R}y \tag{20}$$

and similarly to the case with $n=1$ and $m=2$, the condition (19) is never satisfied.

In this subsection we have demonstrated that for $\mathbf{q}$ in the k_x,k_y plane the linewidth vanishes at small momenta, the intraband contribution vanishes for $|q|<0.008\Gamma M$ while the interband contribution vanishes for $|q|<0.06\Gamma M$. The phonon linewidth along ΓM vanishes for

$$|q| < 0.008\Gamma M \approx 4q_{\text{exp}}. \tag{21}$$

C. Comparison with experiments

In Secs. III B and III A we have analyzed the phonon-linewidth due to the electron-phonon coupling for MgB_2 in the clean limit. We have shown that in this limit this quantity

is zero in an ellipsoid centered at Γ and having axes $q_{\parallel} \approx 0.005 a_0^{-1} \approx 0.4 q_{\exp}^{sd} \approx 4 q_{\exp}$ in the (k_x, k_y) plane and $q_{\perp} \approx 0.052 a_0^{-1} \approx 4 q_{\exp}^{sd} \approx 40 q_{\exp}$ along Γ*A*, where $q_{\exp}^{sd}$ is the Raman momentum transfer for a skin depth of $944.8 a_0$[112] and $q_{\exp}$ is the Raman momentum transfer in the case of an infinite skin depth. Along the Γ-*A* axes $q_{\perp}$ is larger than the largest momenta accessible with Raman scattering. Thus if the Raman experiment is prepared with a geometry consistent with an exchanged momentum along the Γ*A* direction one should indeed find a zero linewidth for the E_{2g} mode. Although this geometry is currently employed[10] in most of the Raman experiments in MgB_2, it seems that a large linewidth (≈40 meV) is detected in the Raman data published up to now. We therefore conclude that the broad feature visible in these experiments cannot be associated to a pure E_{2g} phonon excitations whose linewidth is determined by the electron-phonon coupling of the E_{2g} at $q_{\exp}$. In the final section of the paper we put forward possible explanations for the experimental spectra.

IV. ALLEN FORMULA

The linewidth $\gamma_{\mathbf{q}\nu}$ can be related to the electron-phonon coupling[23] via a simple approximations. Namely, at temperature such that $k_b T \gg \omega_{\mathbf{q}\nu}$ or in the case of a temperature independent $\gamma_{\mathbf{q}\nu}$, using the δ-function condition $\delta(\epsilon_{\mathbf{k}+\mathbf{q}m} - \epsilon_{\mathbf{k}n} - \omega_{\mathbf{q}\nu})$ in Eq. (4) one can substitute in formula (4)

$$\omega_{\mathbf{q}\nu} \frac{f_{\mathbf{k}+\mathbf{q}m} - f_{\mathbf{k}n}}{\omega_{\mathbf{q}\nu}} \mapsto \omega_{\mathbf{q}\nu} \left. \frac{\partial f}{\partial \epsilon} \right|_{\epsilon=\epsilon_{\mathbf{k}n}}. \tag{22}$$

If the temperature dependence in Eq. (4) is weak than the Fermi function can be considered a step function, so that

$$\tilde{\gamma}_{\mathbf{q}\nu} = \frac{4\pi\omega}{N_k} \sum_{\mathbf{k},m,n} |g^{\nu}_{\mathbf{k}n,\mathbf{k}+\mathbf{q}m}|^2 \delta(\epsilon_{\mathbf{k}n}) \delta(\epsilon_{\mathbf{k}+\mathbf{q}m} - \epsilon_{\mathbf{k}n} - \omega). \tag{23}$$

If T_0 is the highest temperature for which the substitution of the derivative of the Fermi function with a Dirac δ function in Eq. (23) is still correct, then Eq. (23) is valid in the range of temperatures such that $k_b T_0 > k_b T \gg \omega_{\mathbf{q}\nu}$. If $\gamma_{\mathbf{q}\nu}$ is temperature independent, then the condition is simply $T < T_0$. It is worth noting that in the limiting case of a very large phonon frequency it might occur that $k_b T_0 < \omega_{\mathbf{q}\nu}$ and formula (23) might never be valid. Since in practice one has phonon frequencies which are of the order of 300 K or more, the only real condition of applicability of Eq. (23) is that $\gamma_{\mathbf{q}\nu}$ has to be temperature independent.

From the definition[30] of the electron-phonon coupling ($\lambda_{\mathbf{q}\nu}$) for the mode ν at point $\mathbf{q}$ one sees that

$$\lambda_{\mathbf{q}\nu} = \frac{\tilde{\gamma}_{\mathbf{q}\nu}}{2\pi N(0) \omega^2_{\mathbf{q}\nu}} \tag{24}$$

which is the Allen formula.[23] The Allen formula allows us to extract the electron phonon coupling from the measured linewidth under the assumption that anharmonic effects are negligible. For MgB_2 this condition is fulfilled along the Γ*A* direction.[7]

In actual calculations, it is customary to neglect the frequency dependence in the δ function in Eq. (23), obtaining

$$\gamma^0_{\mathbf{q}\nu} = \frac{4\pi\omega_{\mathbf{q}\nu}}{N_k} \sum_{\mathbf{k},m,n} |g^{\nu}_{\mathbf{k}n,\mathbf{k}+\mathbf{q}m}|^2 \delta(\epsilon_{\mathbf{k}n}) \delta(\epsilon_{\mathbf{k}+\mathbf{q}m}). \tag{25}$$

This assumption is unjustified at $\mathbf{q}=0$ and leads to the wrong behavior at Γ. Thus formula (25) cannot be used to explain finite temperature Raman experiments due (i) to its (wrong) behavior at Γ and (ii) to the lack of temperature dependence. The correct behaviors are included in expression (4).

V. NUMERICAL CALCULATIONS

A. Model for the electron-phonon coupling matrix element

We consider a model composed of the two σ bands in Eq. (1) coupled to the phonons through a *k*-independent coupling. The electron phonon matrix element is $g_{\mathbf{k}m,\mathbf{k}+\mathbf{q}n} = g\delta_{m,n} + \alpha g(1-\delta_{mn})$, where m, n run over the two σ bands and α determines the magnitude of the interband transitions ($\alpha=0$ correspond to the case where interband transition are suppressed). We assume only one dispersionless phonon mode whose phonon frequency is determined from the calculated E_{2g} phonon frequency at Γ,[7] namely, $\omega_{\mathbf{q}}=65$ meV $=754$ K. Along the Γ*A* direction, as confirmed by inelastic x-ray scattering data,[7] this approximation is fairly correct for the E_{2g} mode. Considering only one phonon mode, from now on we drop the index ν from the linewidth definitions. In the following subsections we calculate the real [Eq. (3)] and imaginary [Eq. (4)] parts of the phonon self-energy [Eq. (2)] in the k_x, k_y plane and along the Γ*A* direction. Technical details on the numerical calculation of the phonon self-energy are given in the Appendix.

B. Phonon self-energy due to the electron-phonon coupling

1. Effect of the band-dispersion along k_z

In the (k_x, k_y) plane, the band structure of Eq. (1) is composed of two bands each of them formed by a free-electron-like dispersion. As a consequence in the $t_{\perp}=0$, $\alpha=0$, and $T=0$ K case (purely two dimensional with noninteracting bands and at zero temperature) one expects to find two singularities (one for each band) at $2k_F$ in the imaginary part of the phonon self-energy and in the first derivative of the real part of the phonon self-energy.

This is shown in Figs. 3(a) and 3(b) (dashed lines) for the real and imaginary parts, respectively. In the real part the singularities in the first derivative are seen as cusps at $2k_F$. At $T=0$ the slope on the right of each cusp should be infinite. A finite slope is obtained as long as a finite nonzero temperature is used[33] (even for small temperatures the slope at $2k_F$ is not vertical). These singularities are originated by the behavior of the response function in two dimensions at $T=0$ and are smoothed out at finite temperature.[33] In three dimensions ($t_{\perp} \neq 0$) the singularities should disappear.[33,34] The real part becomes continuous with no cusps and in the imaginary part the singularities are replaced by smeared continuous peaks. The level of smearing is determined by the three dimensional

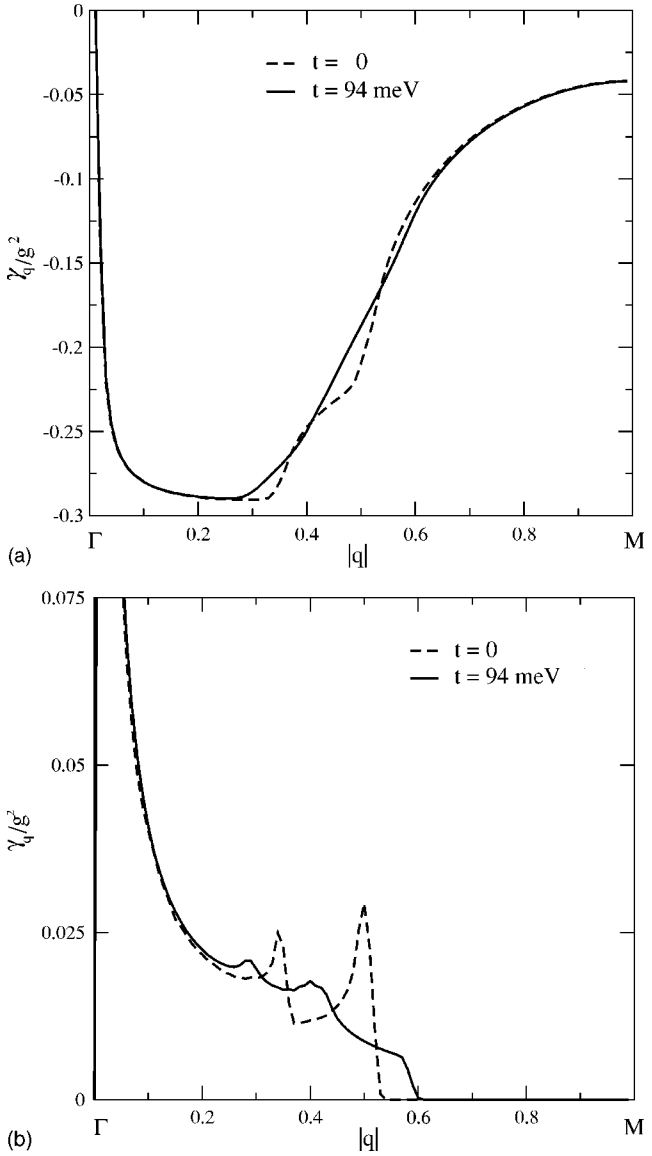

FIG. 3. Real (a) and imaginary (b) part of the phonon self-energy of the E_{2g} mode for $t_\perp=0$ (dashed lines) and $t_\perp=94$ meV (continuous line) calculated for $\mathbf{q}$ along the ΓM direction and at $T=40$ K. Interband transition have been suppressed.

character of the system, in our case by the strength of $t_\perp$. Since the sigma bands in MgB_2 have a small $t_\perp$ it is important to determine how far is the system from the two-dimensional case.

As can be seen in Figs. 3(a) and 3(b) (continuous line) the singularities are strongly affected even in the case of a small $t_\perp$. Indeed the real part presents only very smeared cusps corresponding to the three-dimensional $2k_F$ positions. Similarly the imaginary part presents two smeared peaks at $2k_F$. Even the small $t_\perp$ considered in this paper is sufficient to basically eliminate the effects of the two-dimensional $2k_F$ singularities.

We also study the behavior of the phonon linewidth along the ΓA direction for $t_\perp \neq 0$. Along this direction, the phonon linewidth vanishes for $|\mathbf{q}|<0.1\Gamma A$, as demonstrated in Sec. III A. This is confirmed by the numerical calculations reported in Fig. 7 (continuous line). The phonon linewidth increases monotonically approaching $\mathbf{q}_0=0.1\Gamma A$ from larger momenta and becomes singular for $\mathbf{q}\rightarrow\mathbf{q}_0^+$, due to the behavior caused by the δ function in Eq. (4).

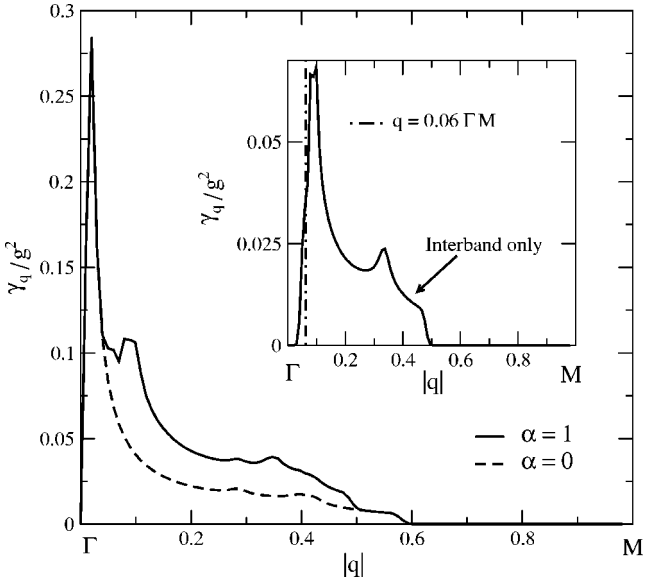

FIG. 4. Imaginary part of the phonon self-energy of the E_{2g} mode calculated at $T=40$ K for $\mathbf{q}$ along the ΓM direction and at $T=40$ K using formulas (3) and (4) for the real and imaginary part, respectively. $\alpha=0$ corresponds to the absence of interband transition. Inset: Intraband contribution to the E_{2g} phonon linewidth. The dashed lines is $q=0.06\Gamma M$, the limit derived analytically in Sec. III B for the vanishing of intraband transition.

2. Effect of the interband transitions between the σ bands

In this section we consider the effect of interband transitions, choosing $\alpha=0,1$ and $t_\perp=94$ meV. The calculated imaginary part of the phonon self-energy at $T=40$ K is illustrated in Fig. 4. In addition to the $2k_F$ features found in the $\alpha=0$ case we found several other features which originates from the interband contribution. The interband contribution drops to zero at $q\approx 0.06\Gamma M$, as was predicted in Sec. III B and as shown in the inset of Fig. 4.

Along the ΓA direction the interband transitions are completely negligible. This can be seen in Fig. 7 where the two curves with $\alpha=1$ and $\alpha=0$ are indistinguishable on the scale of the picture.

3. Temperature effects

In addition to a finite dispersion along the k_z axis, a second effect responsible for the smearing out of the singular features at $2k_F$ is the finite temperature.

In Fig. 5 we show the phonon linewidth for momenta along ΓM for $T=40$ K and $T=300$ K. Overall there is a very weak dependence on temperature. Finite temperature effects (between 40 and 300 K) in the (k_x,k_y) plane are larger close to the $2k_F$ singularities (see inset of Fig. 5). Nevertheless, when compared to the value of the phonon linewidth, temperature effects are fairly small and negligible in the calcu-

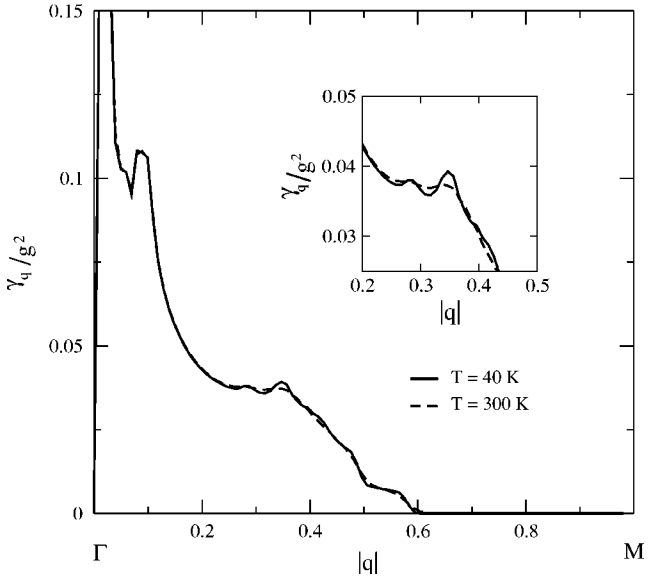

FIG. 5. Imaginary part of the phonon self-energy of the E_{2g} mode calculated at $T=300$ K and $T=40$ K for $\alpha=1$ and $\mathbf{q}$ along the ΓM direction using Eq. (4).

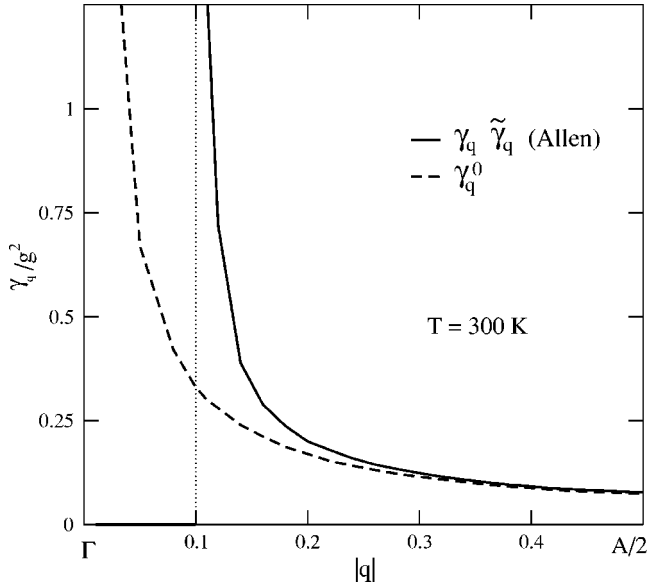

FIG. 7. Phonon linewidth at $T=300$ K for q along the ΓA direction. The $\alpha=1$ case is overlapped to the $\alpha=0$ one, the contribution from intraband transition is very small. The linewidth vanishes for $q \leqslant 0.1\Gamma A$ (dotted line).

lations of the phonon linewidth. Moreover, as can be seen clearly in the inset of Fig. 5, the singular behavior of the two-dimensional $2k_F$ feature is completely lost. For the ΓA direction the effect is even smaller, indeed the results of the calculations at $T=40$ K and $T=300$ K are indistinguishable on the scale of Fig. 7.

4. Reliability of Allen formula

In Figs. 6 and 7 we compare the linewidth calculated using $\gamma_{\mathbf{q}}$ [Eq. (4)], $\tilde{\gamma}_{\mathbf{q}}$ [Eq. (23)], and $\gamma^0_{\mathbf{q}}$ [Eq. (25)] along the ΓM direction and ΓA direction, respectively. In passing from the $\gamma_{\mathbf{q}}$ to $\tilde{\gamma}_{\mathbf{q}}$ we have assumed the linewidth to be temperature independent. In the preceding section (Sec. V B 3) we have shown that this is indeed the case, so that we expect $\gamma_{\mathbf{q}} \approx \tilde{\gamma}_{\mathbf{q}}$ almost everywhere in the Brillouin zone. This is what is seen in Figs. 6 and 7. These two pictures justify the use of the Allen formula for MgB_2.

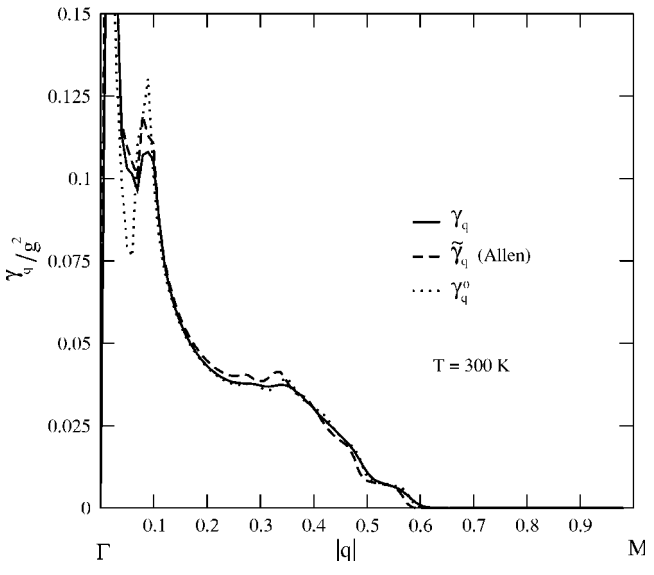

FIG. 6. Phonon linewidth of the E_{2g} mode calculated at $T=300$ K and $\alpha=1$ for $\mathbf{q}$ along the ΓM direction using Eq. (4) ($\gamma_{\mathbf{q}}$), Eq. (23) ($\tilde{\gamma}_{\mathbf{q}}$), and Eq. (25) ($\gamma^0_{\mathbf{q}}$).

From $\tilde{\gamma}_{\mathbf{q}}$, $\gamma^0_{\mathbf{q}}$ is obtained by neglecting the phonon frequency in one of the two δ functions of Eq. (23). This approximation leads to unpredictable results which, as a consequence, must be investigated case by case, since the magnitude of the effects produced by this approximation crucially depends on details of the band structure close to the Fermi level and on the value of the phonon frequency.

As shown in Fig. 6, for $\mathbf{q}$ along the ΓM direction this approximation is fairly well justified. On the contrary along ΓA (see Fig. 7) $\gamma_{\mathbf{q}}$ and $\gamma^0_{\mathbf{q}}$ display two completely different behaviors. This is mainly due to the fact that $\gamma_{\mathbf{q}}$ is singular at $0.1\Gamma A$, while $\gamma^0_{\mathbf{q}}$ is singular for $\mathbf{q} \to 0$ (see Sec. III A). Moreover, as we have shown in Sec. III $\gamma_{\mathbf{q}}=0$ for $q<0.1\Gamma A$. The proper behavior is recovered in the region $0.3\Gamma A<|q|<0.5\Gamma A$, where we find that $\gamma^0_{\mathbf{q}} \approx \gamma_{\mathbf{q}}$.

VI. CONCLUSIONS

In this work we have studied the behavior of the phonon self-energy of the E_{2g} mode, both in its real and imaginary part. Our conclusions can be summarized in the following three points.

(1) *Suppression of Fermi surface singularities in phonon dispersion and linewidth*. Two-dimensional systems display $2k_F$ singularities in the phonon spectrum and linewidth. Naively one would expect MgB_2 to be similar, being the band dispersion along the k_z axis very small. On the contrary we have shown in Sec. V B 1 that even such a small $t_\perp$ strongly suppress the $2k_F$ singularities, so that the phonon spectrum

becomes rather smooth, and the singularities in the phonon linewidth are removed. An additional effect (see Sec. V B 3) is given by finite temperature which at 300 K completely washes out any feature in the imaginary part of the phonon self-energy.

(2) *Behavior of the phonon linewidth for* $\mathbf{q}\rightarrow\Gamma$. We have shown that in the clean limit the phonon linewidth, both in its intraband and interband contributions, vanishes in an ellipsoid centered at Γ and having axes $q_{\parallel}=0.008\Gamma M$ in the (k_x,k_y) plane and $q_{\perp}=0.1\Gamma A$ along the k_z axis (threshold for Landau damping). The two values are larger than the Raman momentum, namely, $q_{\parallel}\approx 0.4q_{\mathrm{exp}}^{sd}\approx 4q_{\mathrm{exp}}$ and $q_{\perp}\approx 4q_{\mathrm{exp}}^{sd}\approx 40q_{\mathrm{exp}}$, where q_{exp}^{sd} is the Raman momentum transfer for a skin depth of $944.8a_0^{-1}$ (Ref. 12) and q_{exp} is the Raman momentum transfer in the case of an infinite skin depth. This calculation demonstrates that the huge linewidth seen in Raman experiments cannot be attributed to the E_{2g} mode.

(3) *Temperature dependence in* $\gamma_{\mathbf{q}\nu}$ *and reliability of the Allen formula* $\tilde{\gamma}_{\mathbf{q}\nu}$ *and of* $\gamma_{\mathbf{q}\nu}^{0}$. The phonon linewidth is almost temperature independent in the $T=0-300$ K region. Small temperature effects are detected close to $2k_F$, but always less than some percent of the total linewidth. Since the phonon linewidth is basically temperature independent the use of the Allen formula $\tilde{\gamma}_{\mathbf{q}\nu}$ is justified in the full Brillouin zone. On the contrary the approximations customary employed in *ab initio* calculations of neglecting the phonon frequency in one of the δ functions in $\tilde{\gamma}_{\mathbf{q}\nu}$, obtaining $\gamma_{\mathbf{q}\nu}^{0}$ is not always justified. Along the Γ-A directions the neglecting of the phonon frequency in the δ function shifts the singularity at $q\approx 0.1\Gamma-A$ to the Γ point, leading to a completely wrong behavior which affects all the region with $q<0.3\Gamma A$.

VII. CONSEQUENCES FOR THE INTERPRETATION OF RAMAN SPECTRA

An immediate result of these three points is that the interpretation of the broad feature seen in Raman spectra at 77 meV (Refs. 10 and 14–19) as a phonon excitation due to the E_{2g} mode at Γ is not correct. Indeed we have shown in this work that the huge temperature dependence of the Raman linewidth cannot be explained by a temperature effect in the electron-phonon contribution to the phonon linewidth. In a preceding work[35] we showed that the anharmonic contributions to the phonon linewidth has a weak temperature dependence. As a consequence the temperature dependence found in Raman data remains completely unexplained. In addition to its temperature dependence, the value of the Raman linewidth at Γ is not consistent with the theoretical findings. Indeed we have demonstrated that electron-phonon contribution to the phonon linewidth is zero in an ellipsoid centered in Γ and larger than the Raman exchanged momentum. This is not at all the case for what concerns Raman spectra.

There are additional considerations, concerning the position of the 77 meV feature, which seem to indicate that it is very unlikely that it can be interpreted as due to a phonon excitation at Γ. The calculated harmonic phonon frequency of the E_{2g} mode at Γ is indeed 65 meV, a value 15% smaller than the experimental result. This has led several groups to the conclusion that the difference might be due to anharmonic effects.[4,27,36,37] A careful determination[35] of the anharmonic phonon frequency shift, explicitly taking into account three and four phonon vertexes and the scattering between different phonon modes at different q points in the Brillouin zone gives a fairly small value of this quantity at Γ (+5% of the harmonic phonon frequency, $\approx$3.12 meV), clearly too small to justify the feature at 77 meV. This is confirmed by inelastic x-ray data of two independent groups[7,8] showing phonon spectra in good agreement with the harmonic phonon frequencies, suggesting small anharmonic effects. Unfortunately inelastic x-ray scattering is not possible at the zone center, so that a direct comparison of the spectra cannot be performed.

In what follows we analyze several hypotheses that can be made in order to reconcile, theory and inelastic x-ray data with experiments with Raman data. A possibility is that the 77 meV feature in Raman data could be ascribed to a single resonant process involving the E_{2g} phonon mode coupled to electronic excitations. This would be consistent with the asymmetric shape of the peak, reminiscent of a Fano resonance.[38] As a consequence the position of the peak would not correspond to the E_{2g} mode phonon frequencies but it would be slightly shifted to lower frequencies. The temperature dependence of the linewidth might be different in this case. In this case it is interesting to study the peak position as a function of the energy of the incident light. A study of the dependence of the spectrum from the wavelength of the incident light has been performed in Ref. 14. It is shown that as the wavelength is changed, the peak energy position remains basically the same, even if the shape changes substantially. In the same work, from the study of the depolarization ratio between parallel and perpendicular orientations of the incident and emitted light, it is concluded that the symmetry of the excitation *cannot* be that of a single E_{2g} mode, supporting the idea illustrated in this paper that the Raman does not measure the E_{2g} phonon excitation at Γ.

An alternative scenario is that the Raman peak might be due to excitation of phonons which are not at the Γ point. Such an excitation can be activated by (i) the presence of defects such as Mg vacancies, and (ii) multiphonon scattering. A defect breaks translational symmetry and it makes possible to observe in Raman spectra phonon excitations at nonzero momenta. Indeed in a similar system such as defected Graphite, due to the almost two dimensional character of the electronic structure and a strong electron-phonon coupling,[39,40] the phonon at the K-zone boundary has a very strong signal in Raman spectra (known as the D peak).

However, impurities scattering alone cannot explain the strong temperature dependence of MgB_2 Raman linewidth between 40 and 300 K. This temperature range is not high enough to change the population of a phonon at 77 meV. The temperature dependence might be explained by a multiphonon process such as the absorption of an acoustic phonon and emission of an optical phonon with opposite nonzero momenta. Multiphonon scattering is also seen in graphite[41] and is responsible for the G' peak observed in Raman spectra.

Finally there is an additional mechanism that could explain the absence of a Landau threshold in MgB_2. Indeed it

has been suggested[28] that, in the presence of impurities and in the dirty limit, there is no threshold for Landau damping. However also this mechanism is temperature independent and therefore not compatible with the strong temperature dependence of MgB_2 Raman spectra. Moreover it is not yet clear if the MgB_2 single crystals are in the clean or dirty limit.[42] Therefore additional work is necessary to determine if this effect is relevant in MgB_2 single crystals.

ACKNOWLEDGMENTS

We acknowledge illuminating discussion with A. Shukla, M. d'Astuto and A. C. Ferrari and I. Mazin. The calculations were performed at the IDRIS supercomputing center (Project No. 031202).

APPENDIX: TECHNICAL DETAILS

In the calculations of the real part of the phonon self-energy along ΓM we consider a finite temperature and we implement Eq. (2) with a η smearing of 350 K. This smearing is necessary to calculate the principal value in Eq. (2). Thus we extract the real part at the end. This procedure gives a faster convergence as a function of N_k. The sums are performed using a grid of $N_k = 300 \times 300$ for the two-dimensional case with $t_\perp = 0$ and $N_k = 300 \times 300 \times 300$ for the three-dimensional case with $t_\perp \neq 0$. In both cases the grids are formed by N_k *symmetry-irreducible k* points, obtained from a mesh centered at Γ and randomly displaced from the origin.

In the calculation of the imaginary part we replace the Dirac delta functions with Gaussians of width σ, namely,

$$\delta(x) \rightarrow \frac{e^{-x^2/\sigma^2}}{\sqrt{\pi\sigma}}. \tag{26}$$

We then compute $\gamma_{\mathbf{q}}$, $\tilde{\gamma}_{\mathbf{q}}$, and $\gamma^0_{\mathbf{q}}$ [using Eqs. (4), (23), and (25), respectively] as a function of σ on a given mesh of N_k *symmetry-irreducible k* points. We then repeat the calculation on grids with always higher N_k (with N_k up to $300 \times 300 \times 300$) in order to perform the limits of $N_k \rightarrow \infty$ and $\sigma \rightarrow 0$. In this way we obtain the continuum limit. The comparison between the results for the phonon linewidth obtained using the different formulas allows to judge the reliability of the different approximations in the calculation of the phonon linewidth.

In Figs. 8(a) and 8(b) we show the convergence of the linewidths $\gamma_{\mathbf{q}}$ ($\mathbf{q} = 0.6\Gamma A$) as a function of the Gaussian smearing σ (expressed in K). In (a) we used a Gaussian smearing, in (b) an Hermitian-Gaussian smearing of order 1.[20] As can be seen, the dependence on the smearing is fairly weak for the largest mesh ($N_k = 27 \times 10^6$). In this case the calculation is converged for $\sigma > 50$ K. Moreover the phonon linewidth is weakly dependent on σ for $\sigma < 600$ K. We adopt this mesh and σ included between 50–100 K in the calculations.

Note that previous *ab initio* calculations of the phonon linewidth[7] have been performed with mesh of 27000 symmetry-irreducible *k* points. For the case of an Hermite Gaussian smearing, as can be seen in the picture, this would lead to an error in the estimation of the phonon linewidth of the order of $\approx 5\%$.

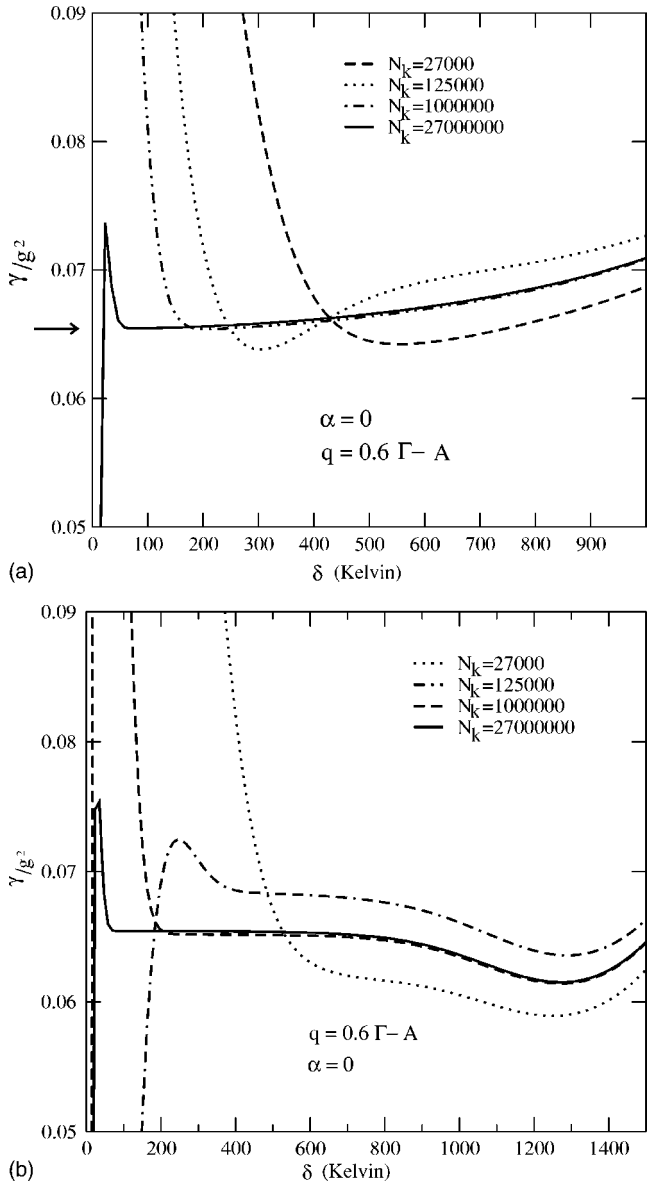

FIG. 8. Phonon linewidth calculated at $T = 300$ K using formula (4) as a function of the Gaussian smearing (σ), of the number N_k of *k* points used in the sum. The arrow indicates the value that can be extracted from the largest mesh calculation. In (a) a pure Gaussian smearing has been used, while in (b) an Hermite-Gaussian smearing of order 1.

It is interesting to evaluate the effect of the scattering between electron and impurities on the phonon linewidth.[31] To this purpose one should use a finite values for σ equal to the electron linewidth (the inverse of the electron scattering rate). This quantity in *c*-axis-oriented MgB_2 films has been estimated in the range of 52–400 K (Ref. 32) at a temperature of 45 K. Since in Fig. 8 there is a very weak dependence of the phonon linewidth on σ, for $\sigma < 600$ K, we can conclude that the finite electron linewidth has no observable effects on the phonon linewidth.

[1] J. Nagamatsu, N. Nakagawa, T. Muranaka, Y. Zenitani, and J. Akimitsu, Nature (London) **410**, 63 (2001).
[2] J. M. An and W. E. Pickett, Phys. Rev. Lett. **86**, 4366 (2001).
[3] K. D. Belashchenko, M. van Schilfgaarde, and V. P. Antropov, Phys. Rev. B **64**, 092503 (2001).
[4] J. Kortus, I. I. Mazin, K. D. Belashchenko, V. P. Antropov, and L. L. Boyer, Phys. Rev. Lett. **86**, 4656 (2001).
[5] Y. Kong, O. V. Dolgov, O. Jepsen, and O. K. Andersen, Phys. Rev. B **64**, 020501(R) (2001).
[6] K. P. Bohnen, R. Heid, and B. Renker, Phys. Rev. Lett. **86**, 5771 (2001).
[7] A. Shukla, M. Calandra, M. d'Astuto, M. Lazzeri, F. Mauri, C. Bellin, M. Krisch, J. Karpinski, S. M. Kazakov, J. Jun, D. Daghero, and K. Parlinski, Phys. Rev. Lett. **90**, 095506 (2003).
[8] A. Q. R. Baron, H. Uchiyama, Y. Tanaka, S. Tsutsui, D. Ishikawa, S. Lee, R. Heid, K.-P. Bohnen, S. Tajima, and T. Ishikawa, Phys. Rev. Lett. **92**, 197004 (2004).
[9] J. M. An, S. Y. Savrasov, H. Rosner, and W. E. Pickett, Phys. Rev. B **66**, 220502(R) (2002).
[10] J. W. Quilty, S. Lee, A. Yamamoto, and S. Tajima, Phys. Rev. Lett. **88**, 087001 (2002).
[11] D. L. Mills, A. A. Maradudin, and E. Burnstein, Ann. Phys. (N.Y.) **56**, 504 (1970).
[12] J. W. Quilty, S. Lee, S. Tajima, and A. Yamanaka, Phys. Rev. Lett. **90**, 207006 (2003).
[13] R. Zeyher, Phys. Rev. Lett. **90**, 107002 (2003).
[14] P. M. Rafailov, M. Dworzak, and C. Thomsen, Solid State Commun. **122**, 455 (2002).
[15] J. Hlinka, I. Gregora, J. Pokorny, A. Plecenik, P. Kus, L. Satrapinsky, and S. Benacka, Phys. Rev. B **64**, 140503(R) (2001).
[16] H. Martinho, C. Rettori, P. G. Pagliuso, N. O. Moreno, and J. L. Sarrao, cond-mat/0105204 (unpublished).
[17] A. F. Goncharov, V. V. Struzhkin, E. Gregorianz, J. Hu, R. J. Hemley, H. K. Mao, G. Lapertot, S. L. Bud'ko, and P. C. Canfield, Phys. Rev. B **64**, 100509(R) (2001).
[18] K. Kunc, I. Loa, K. Syassen, R. K. Kremer, and K. Ahn, J. Phys.: Condens. Matter **13**, 9945 (2001).
[19] X. K. Chen, M. J. Konstantinovic, J. C. Irwin, D. D. Lawrie, and J. P. Franck, Phys. Rev. Lett. **87**, 157002 (2001).
[20] S. de Gironcoli, Phys. Rev. B **51**, 6773 (1995).
[21] The convergence is given by the number of k points in the symmetry-irreducible wedge of the Brillouin zone.
[22] I. I. Mazin and J. Kortus, Phys. Rev. B **65**, 180510(R) (2002).
[23] P. B. Allen, Phys. Rev. B **6**, 2577 (1972); P. B. Allen and R. Silberglitt, *ibid.* **9**, 4733 (1974).
[24] E. Cappelluti, S. Ciuchi, C. Grimaldi, and L. Pietronero, Phys. Rev. B **68**, 174509 (2003).
[25] In *ab initio* calculation $V=V_{KS}$ is the full self-consistent potential which includes correlation effects. For a detailed derivation see P. B. Allen, in *Dynamical Properties of Solids*, edited by G. K. Horton and A. A. Maradudin (North-Holland, Amsterdam, 1980), pp. 95–196.
[26] O. Jepsen, I. I. Mazin, A. I. Liechtenstein, O. K. Andersen, and C. O. Rodriguez, Phys. Rev. B **51**, 3961 (1995).
[27] A. Y. Liu, I. I. Mazin, and J. Kortus, Phys. Rev. Lett. **87**, 087005 (2001).
[28] O. V. Misochko and E. Ya. Sherman, Phys. Rev. B **51**, 1326 (1995).
[29] V. L. Aksenov and V. V. Kabanov, Phys. Rev. B **57**, 608 (1998).
[30] G. Grimvall, *The Electron-Phonon Interaction in Metals* (North Holland, Amsterdam, 1981), p. 201.
[31] E. J. Nicol and J. P. Carbotte, Phys. Rev. B **50**, 10 243 (1994).
[32] J. J. Tu, G. L. Carr, V. Perebeinos, C. C. Homes, M. Strongin, P. B. Allen, W. N. Kang, Eun-Mi Choi, Hyeong-Jin Kim, and Sunk-Ik Lee, Phys. Rev. Lett. **87**, 277001 (2001); F. Marsiglio, *ibid.* **87**, 247001 (2001); E. G. Maksimov, J. Kortus, O. V. Dolgov, and I. I. Mazin, *ibid.* **89**, 129703 (2002); F. Marsiglio, *ibid.* **89**, 129704 (2002).
[33] J. G. Kim, Y. H. S. Choi, E. K. Lee, and S. Lee, Phys. Rev. B **59**, 3661 (1999).
[34] A. L. Fetter and J. D. Walecka, *Quantum Theory of Many-Particle System* (McGraw-Hill, New York, 1971), p. 176.
[35] M. Lazzeri, M. Calandra, and F. Mauri, Phys. Rev. B **68**, 220509(R) (2003).
[36] T. Yildirim, O. Gulseren, J. W. Lynn, C. M. Brown, T. J. Udovic, Q. Huang, N. Rogado, K. A. Regan, M. A. Hayward, J. S. Slusky, T. He, M. K. Haas, P. Khalifah, K. Inumaru, and R. J. Cava, Phys. Rev. Lett. **87**, 037001 (2001).
[37] H. J. Choi, D. Roundy, H. Sun, M. L. Cohen, and S. G. Louie, Nature (London) **418**, 758 (2002); H. J. Choi, D. Roundy, H. Sun, M. L. Cohen, and S. G. Louie, Phys. Rev. B **66**, 020513(R) (2002).
[38] U. Fano, Phys. Rev. **124**, 1866 (1961).
[39] C. Thomsen and S. Reich, Phys. Rev. Lett. **85**, 5214 (2000).
[40] S. Piscanec, M. Lazzeri, F. Mauri, A. C. Ferrari, and J. Robertson, Phys. Rev. Lett. **93**, 185503 (2004).
[41] L. G. Cancado, M. A. Pimenta, R. Saito, A. Jorio, L. O. Ladeira, A. Grueneis, A. G. Souza-Filho, G. Dresselhaus, and M. S. Dresselhaus, Phys. Rev. B **66**, 035415 (2002).
[42] I. I. Mazin, O. K. Andersen, O. Jepsen, O. V. Dolgov, J. Kortus, A. A. Golubov, A. B. Kuz'menko, and D. van der Marel, Phys. Rev. Lett. **89**, 107002 (2002).